The Melting of Highly Oriented Fibre DNA Subjected to Osmotic Pressure

Andrew Wildes,[*,†] Liya Khadeeva,[†,‡] William Trewby,[†,¶,@] Jessica Valle-Orero,[†,△] Andrew Studer,[§] Jean-Luc Garden,[‖,⊥] and Michel Peyrard[*,#]

Institut Laue-Langevin, CS 20156, 71 avenue des Martyrs, 38000 Grenoble, France, Institut de Physique de Rennes, UMR UR1 - CNRS 6251, 35042 Rennes cedex, France, Department of Physics and Astronomy, University College London, Gower St., London WC1E 6BT, UK, ANSTO, Locked Bag 2001, Kirrawee DC, NSW 2232, Australia, CNRS, Institut NÉEL, F-38042 Grenoble, France, Université Grenoble Alpes, Inst NEEL, F-3800 Grenoble, France, and Laboratoire de Physique, Ecole Normale Supérieure de Lyon, 46 allée d'Italie, 69364 Lyon Cedex 07, France

E-mail: wildes@ill.fr; michel.peyrard@ens-lyon.fr

Phone: +33 (0)4 76 20 70 37. Fax: +33 (0)4 76 20 71 20

[*]To whom correspondence should be addressed
[†]Institut Laue-Langevin
[‡]Institut de Physique de Rennes
[¶]University College London
[§]ANSTO
[‖]CNRS Grenoble
[⊥]Université Grenoble Alpes
[#]ENS Lyon
[@]Current address: Centre for Materials Physics, Physics Department, Durham University, Stockton Road, Durham, DH1 3LE, UK
[△]Current address: Columbia University, Biological Sciences, 1011A Fairchild Center, 1212 Amsterdam Av., New York, NY 10027, USA

Abstract

A pilot study of the possibility to investigate the temperature-dependent neutron scattering from fibre-DNA in solution is presented. The study aims to establish the feasibility of experiments to probe the influence of spatial confinement on the structural correlation and the formation of denatured bubbles in DNA during the melting transition. Calorimetry and neutron scattering experiments on fibre samples immersed in solutions of polyethylene glycol (PEG) prove that the melting transition occurs in these samples, that the transition is reversible to some degree, and that the transition is broader in temperature than for humidified fibre samples. The PEG solutions apply an osmotic pressure that maintains the fibre orientation, establishing the feasibility of future scattering experiments to study the melting transition in these samples.

Keywords

DNA,PEG,UV

Introduction

The melting transition for DNA is a process by which the hydrogen bonds between base pairs break as the temperature is increased, eventually leading to the complete separation of the two strands of the double helix. This thermal denaturing of the molecule has been the subject of considerable research, including attempts to describe the transition from a theoretical physics point of view using statistical mechanics.[1]

The experimental techniques used to study the melting transition have, almost exclusively, been either point probes, such as fluorescence, or bulk probes, such as UV absorbance or circular dichroism. These methods are able to determine the percentage of the base pairs that have denatured, but are unable to determine whether there is any spatial correlation between denatured base pairs. A complete understanding of the melting transition requires

the spatial correlation to be accounted for, as cooperative dynamics within the molecule will have a substantial influence on the denaturing of the base pairs.

We have therefore recently begun a program of using scattering methods to study the melting transition.[2–4] Scattering techniques probe the correlation function of the sample, and hence are able to give information on the spatial correlations. This is most effective, however, when the scattering gives clear and strong coherent signals such as Bragg peaks.

It is possible to orient DNA to create samples that will give Bragg peaks. Indeed, the double helix structure of the molecule was determined based on the analysis of X-ray diffraction patterns. Oriented DNA takes the form of fibres, where the molecules adopt a close-packed arrangement. The DNA molecules can adopt a number of configurational forms, depending on the water content of the fibres. This can be controlled by storing the samples in an atmosphere with a given relative humidity. We have studied the temperature dependence of the Bragg peaks from highly oriented A-[4] and B-form[2,3] DNA and have successfully applied a statistical mechanical model[5,6] for the melting transition to the results. A similar study on the melting of non-oriented DNA fibres has also been published.[7]

While the comparisons between the experimental data and the modelling have been satisfactory, obvious concerns arise regarding the effects of spatial confinement on the melting process. The molecules are close-packed within the fibre structure, hence questions may justifiably be asked concerning the influence that the degrees of spatial freedom that the base pairs have for fluctuation, and possible constraints imposed by spatial confinement, might have on the experiment and interpretation.

Using a method that increased the distance between the molecules in a fibre, without losing the orientation required to produce Bragg peaks, would allow the influence of spatial confinement on the melting transition to be investigated. Putting the fibres into water and applying osmotic pressure by means of a long chain molecule may be such a method. Podgornik, Rau, Parsegian and co-workers[8–11] have published a substantial number of articles showing that immersing fibre DNA in polyethylene glycol (PEG) solutions will apply suffi-

cient pressure to maintain a fibre structure while allowing the fibre to swell and increase the distance between the molecules within the fibres.

DNA in water/PEG solutions have also been used as model systems for studying the effects of crowding on the dynamics and the configurational forms of DNA.[12–14] They are of interest as they may reproduce conditions within the cell, where spatial constraints imposed by DNA folding and osmolytes will be important. DNA in PEG solutions will undergo a melting transition, and a number of studies have been performed to establish the dependence of the melting transition on the PEG length and the salinity of the solution.[15–18] All the published studies to date on the melting of DNA in PEG solutions have been on non-oriented DNA and give limited information, if any, on the spatial correlations along molecule.

A fundamental question in these studies concerns the interaction of the DNA with the PEG during melting, particularly whether the PEG might bind with a broken hydrogen bond between base pairs. This may be the case for small PEG molecules, however it is believed that the influence of larger PEG molecules (with molecular weight, MW, > 1000) is through limiting the available space for DNA configurations, i.e. through confinement and excluded volume.[12,13,15,18] Larger PEG molecules with MW ≥ 8000 with sufficient concentration also do not penetrate a highly oriented fibre sample,[9] meaning that any PEG-DNA interaction would be limited to the surface of the fibre and any observed confinement effects would be dominated by the distance between DNA molecules. The use of water/PEG solutions could therefore be an elegant way to study the effects of confinement on the spatial correlations in the melting of DNA.

We present here a pilot study to determine whether it is possible to perform temperature-dependent diffraction measurements of fibre DNA subjected to osmotic pressure.

Experimental methods

Sample preparation.

The samples were made using commercially available salmon testes DNA purchased from Sigma Co. Highly oriented fibre samples of Na-DNA were made using the "wet spinning" technique.[19,20] The method and the concentrations for the DNA solution and spinning bath are the same as has been reported in previous publications.[21,22]

Once prepared, the fibres were initially stored in an atmosphere humidified to 56 % ^2H_2O by means of an oversaturated salt solution. One group of fibres was subsequently humidified to 92 %, which would nominally cause it to take the B-form conformation.[22] This sample group is hereafter defined as "Dry".

Solutions of 20,000 MW polyethylene glycol (PEG) were made for the osmotic pressure samples. The PEG was dissolved in a solution of ^2H_2O with 0.5 M NaCl, 10 mM Tris and 1 mM EDTA with pH 7. The choice for the solution was based on previous work by Podgornik *et al.*[10] which established that PEG of this size with concentrations > 7 % (wt/wt) does not penetrate into the fibre.

A fibre sample immersed in a PEG solution of 10 % (wt/wt) was prepared for the calorimetry measurements. The calorimetry was measured for both this sample, and a "dry" sample for comparison.

PEG solutions of 17 %, 26 % and 40 % (wt/wt) were prepared for the neutron scattering measurements, corresponding to osmotic pressures[23] of 6.5, 7.0 and 7.5 dyne·cm^2. These concentrations were chosen based on the pressure-DNA concentration figure shown by Podgornik *et al.*[10] The figure shows two regimes. The DNA concentration scales linearly with the logarithm of the osmotic pressure in each regime, but with a different gradient. The two regimes were linked to the intermolecular ordering in the fibre, and potentially to the transition between bond orientational ordering and a cholesteric phase. The 40 % PEG solution corresponds to the high pressure regime, the 17 % solution to the low pressure regime, and

the 26 % solution to the boundary between the two.

The incoherent scattering cross-section for neutrons is very large for samples containing protonated hydrogen, creating a large background that can mask a weak signal. It was for this reason that deuterated water was used for humidification and for preparation of the PEG solutions. The hydrogens on the DNA and the PEG will not easily exchange, however, and the incoherent background was expected to be large.

All the fibres were concertina folded and placed with their axes co-aligned in square aluminium cassettes. The dimensions of the sample in the cassettes were roughly 20 × 20 × 2 mm^3 and the total fibre mass for each was roughly 0.6 g. The cassettes were sealed using lead wire. The "dry" sample was sealed in its 92 % RH atmosphere. The cassettes containing the remaining samples were each filled with approximately the same volume of either the 17 %, 26 % or 40 % PEG solution just before being sealed. The samples were left to equilibrate with the liquid for a week before being measured.

Differential scanning calorimetry

Calorimetry measurements were made using a Seratam Micro DSC III. A sample was placed in a Hastelloy tube for each of the experiments. The tube was sealed to conserve the water content during the measurement. The differential heat flux was measured relative to an empty reference tube. The sample was placed in the calorimeter at an initial temperature of 293 K and then cooled to 268 K. After 10 minutes at this temperature, the sample was heated and the differential heat flux recorded. The heating and cooling rates for all the measurements was 0.6 $K \cdot min^{-1}$.

The heat capacity, ΔC, was calculated from the differential heat flux, ΔP, using the equation:

$$\Delta C = \left(\Delta P + \tau \frac{\mathrm{d}\Delta P}{\mathrm{d}t} \right) \cdot \frac{\mathrm{d}t}{\mathrm{d}T}, \tag{1}$$

where T is temperature and t is time. The instrument response constant for the instrument,

τ, was 60 s. The specific heat was then calculated by:

$$\Delta c = \frac{\Delta C}{m}, \tag{2}$$

where m is the sample mass. The mass of the "dry" sample was 0.152 g, and the total mass (fibre and solution) of the 10 % PEG sample was 0.057 g.

Previous calorimetry measurements show that the melting transition is an irreversible process in humidified (or, in the context of this article, "dry") fibres.[2–4] The PEG sample was subjected to a thermal cycle to test whether the same was true for a sample subjected to osmotic pressure. After measuring the calorimetry while heating to 383 K, this temperature was maintained for 5 minutes and then the sample was cooled back to 268 K. The calorimetry measurement was then repeated. This heating/cooling cycle was run a total of four times.

Neutron scattering

The samples were measured using the WOMBAT powder diffractometer at the Bragg Institute, Australia.[24] The instrument was configured with a germanium monochromator. Higher order Bragg contamination was suppressed using a room temperature beryllium filter. WOMBAT has a position-sensitive detector that covers 120° in the scattering plane with an oscillating radial collimator for background suppression.

Figure 1 shows the scattering geometry for the neutron scattering experiments. The incident beam with wavevector $\mathbf{k_i}$ was scattered through an angle 2θ into the final direction with wavevector $\mathbf{k_f}$ and a corresponding momentum transfer to the sample of $\mathbf{Q} = \mathbf{k_i} - \mathbf{k_f}$. The scattering was measured in transmission through the sample cassette. The WOMBAT detector position was fixed for the measurements, and the sample was rotated about the axis normal to the scattering plane. The scattering was plotted relative to a previously used convention defining orthogonal reciprocal space directions $\mathbf{Q_H}$, $\mathbf{Q_K}$ and $\mathbf{Q_L}$.[22] Figure 1 also shows the axes H, K and L, which are given relative to the geometry of the square cassette.

The H axis is parallel to the fibre axis, the L direction is perpendicular to the fibre axis and in the plane of the cassette and K is normal to the cassette.

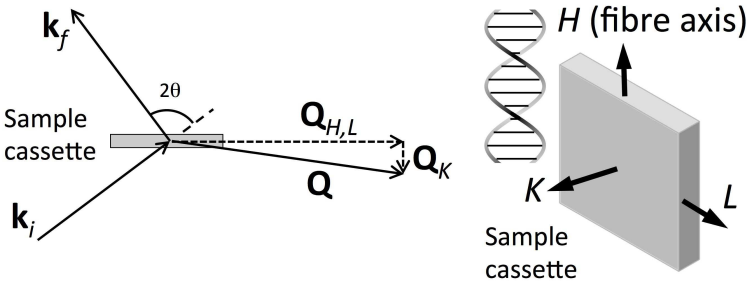

Figure 1: (left) Schematic showing the neutron scattering geometry. The scattering was measured in transmission through the sample cassette, with the fibre axis either in (thus measuring in the (Q_H, Q_K) plane) or normal to (thus measuring in the (Q_L, Q_K) plane) the scattering plane. (right) Schematic showing the definition of the H, K and L axes relative to the sample cassette. The DNA molecules are parallel to the fibre axis, which is defined as the H direction.

Two sets of measurements were made:

The first used a wavelength of 5.65 Å, which allowed reciprocal space maps to be measured for all the samples from $0.3 \lesssim Q \lesssim 2$ Å^{-1}, where Q is the magnitude of $\mathbf{Q}$. This Q range adequately covers the observable Bragg features in neutron scattering from B-form DNA.[22] Reciprocal space maps were measured with the fibre axis (H) within and normal to the scattering plane. These measurements were all made at room temperature.

The second used a wavelength of 4.61 Å and focused on the temperature dependence of the prominent Bragg peak at $\mathbf{Q_H} \approx 1.87$ Å^{-1} along the fibre axis. The temperature was controlled between 300 and 380 K using jets of heated nitrogen gas and the temperature stability for the duration of each measurement was < 0.1 K. The samples were considered to be in thermal equilibrium at each temperature.

Results

Differential scanning calorimetry

The measured specific heat, Δc, for the "dry" sample is shown in figure 2. The melting transition occurs close to 85°C and its temperature range is quite narrow. The results are qualitatively very similar to the melting transition observed in other "dry" fibres.[22]

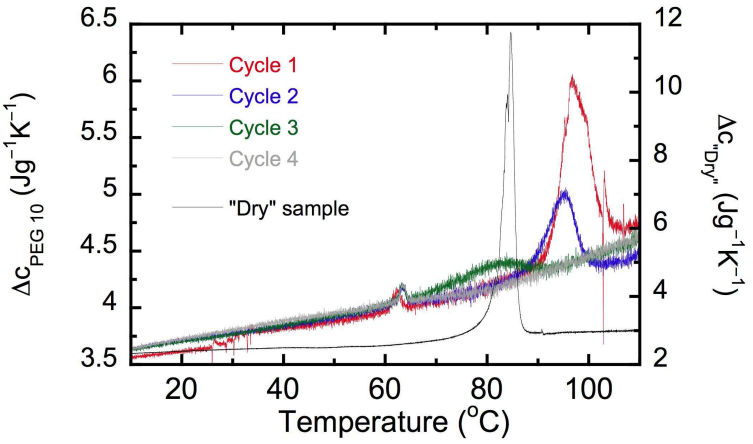

Figure 2: Specific heat, Δc, for a 92 % RH "dry" Na-DNA sample (right hand scale), and from multiple thermal cycles for the same type of sample in a 10 % PEG solution (left hand scale).

The figure also shows Δc for the thermal cycles of the 10 % PEG sample. The transition shows some reversibility in this sample. The specific heat shows a clear peak in the first temperature ramp, corresponding to the melting temperature, which is at a higher temperature than that for the "dry" sample and whose width is substantially broader. A peak is also observed in the second temperature ramp, indicating some reversibility in the melting transition. The peak is reduced in amplitude and the melting temperature is closer to that for the "dry" sample, although the peak width is similar to that for the first ramp. The peak is much reduced in amplitude and melting temperature in the third ramp, and the width is substantially broader. No clear peak is observed in the fourth ramp.

The data show that the melting transition is observable in highly oriented fibre samples subjected to osmotic pressure. The PEG solution clearly has some influence on the transition,

affecting the melting temperature, the peak shape and giving a degree of reversibility. The results indicate that spatial confinement of the DNA molecules has an influence on the melting transition.

Reciprocal space maps

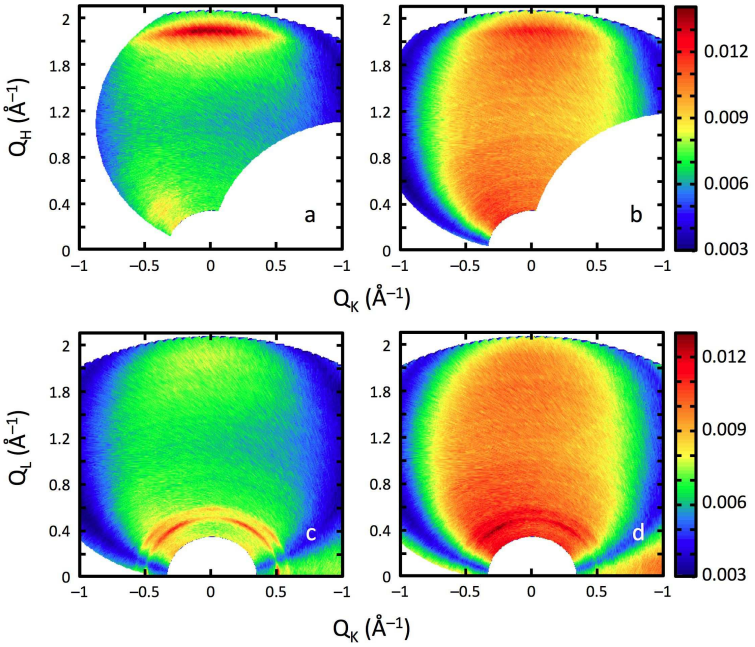

Figure 3: Reciprocal space maps of different scattering planes for the "dry" (a, c) and PEG 17 (b, d) fibre DNA samples. Figures (a) and (b) are on the same intensity scale, shown by the colour bar to the right of (b). Likewise, (c) and (d) are on the same scale.

Examples of the reciprocal space maps are shown in figures 3. Figures 3(a) and (c) show the maps for the "dry" sample with the fibre axis respectively within and normal to the scattering plane. The data show that this sample, as expected, is in B-form. Figure 3(a) shows a prominent Bragg peak along the fibre axis, centered at $Q_H \approx 1.87$ Å^{-1}. The figure also shows a feature at $(Q_H, Q_K) \sim (0.3, -0.3)$, where a weaker Bragg peak is also expected for B-form.[22] Figure 3(c) shows the map with the fibre axis normal to the scattering plane. Well-defined features are observed at small $|Q|$, similar to those observed in previous studies including small angle scattering measurements from fibre samples in PEG solutions.[10] These features are frequently used to gauge the intermolecular spacing.

The data show a dip in the intensity, giving rise to a feature resembling a (blue) halo in the maps. This is due to attenuation when either the incident or the scattered beam was in the plane of the aluminium cassette. The halo dip is relatively localised, but does influence the intensity close to the $Q_H \approx 1.87$ Å^{-1} Bragg peak at this wavelength.

The PEG samples all showed very similar results, and only the 17 % PEG maps are shown in figures 3(b) and (d). The data are qualitatively the same as those for the "dry" sample for both the measured orientations, with the prominent Bragg peak at $Q_H \approx 1.87$ Å^{-1} and features at small $|Q|$ in the $Q_{K,L}$ plane. The features are smaller in magnitude and may be broader in sample rotation angle, suggesting that some orientation of the fibres has been lost. The PEG samples have substantially more incoherent scattering than the "dry" sample due to the presence of a significant amount of protonated PEG. Nevertheless, the presence of the Bragg peaks proves that the samples have maintained the B-form and that a decent fraction retains the oriented fibre structure.

Figure 4(a) shows cuts in the maps along the Q_H direction at $Q_{KL} = 0$. The two datasets share the same intensity scale. The "dry" sample shows a clear, Lorentzian-like Bragg peak with a peak amplitude that is roughly twice the incoherent background. The 17 % PEG sample also shows a clear peak at the same position, meaning that the pitch of the DNA helix has remained unchanged. The background is larger by 50 % and the peak signal-to-noise is reduced to ≈ 0.2. The peak may also be asymmetric, with the suggestion of a broad hump on the low-Q side of the peak. Intensities on the high-Q sides of the peaks are unreliable at this wavelength due to the beam attenuation halo.

The data in figures 3(c) and (d) may be plotted as a function of the magnitude of the momentum transfer, $|Q_{K,L}|$, by summing the intensity measured at equivalent scattering angles, 2θ, and converting the axis to $Q = 4\pi \sin\theta/\lambda$. The resulting plot, shown in figure 4(b), may then be used to judge the influence of the PEG solution on the intermolecular spacing. The "dry" sample shows clear Bragg peaks at $|Q_{K,L}| \sim 0.5$ and 0.575 Å^{-1}. The corresponding peaks are at $|Q_{K,L}|$ values that are roughly 2 % smaller, equivalent, and 4 %

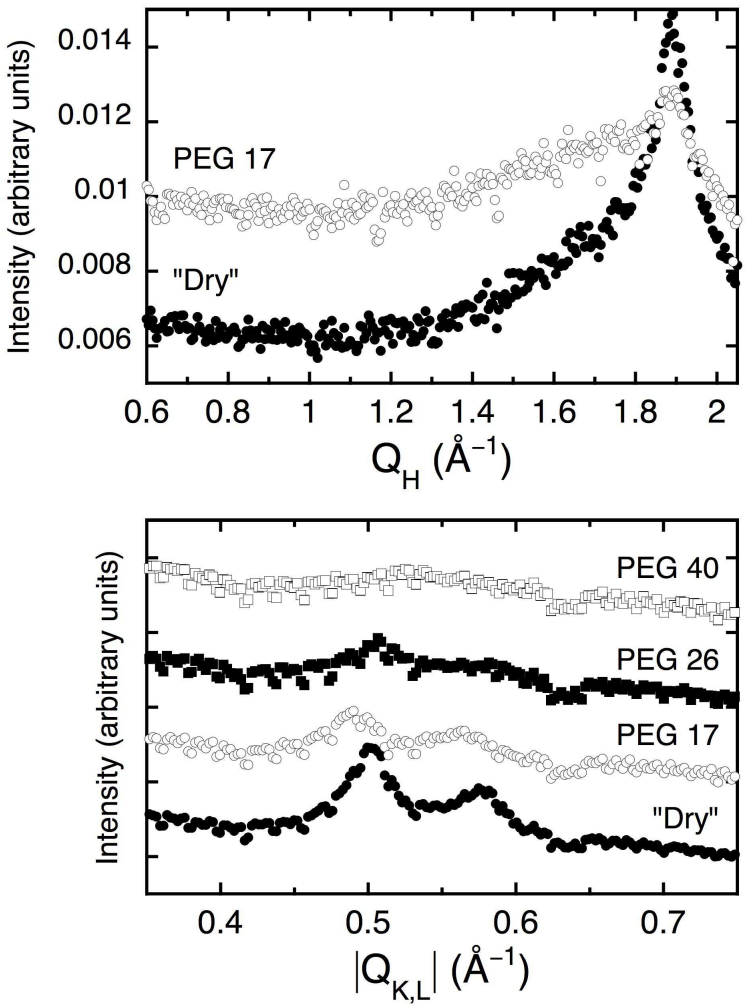

Figure 4: (a) Cuts along the Q_H axis through the reciprocal space maps shown in figures 3 (a) and (b). The intensities are shown on the same scale. (b) The intensities in figures 3 (c) and (d), integrated for constant scattering angle and hence plotted as a function of $|Q_{K,L}|$. The "dry" and PEG 17 samples are plotted on the same scales, while the PEG 26 and PEG 40 have been shifted vertically to distinguish them from the PEG 17 data.

larger than the "dry" sample for the 17 %, 26 % and 40 % PEG samples respectively. This implies that the 17 % PEG samples have indeed swollen relative to their "dry" counterparts, with larger intermolecular spacing and while maintaining an oriented fibre form. The 26 % PEG sample has roughly the same intermolecular spacing, while the DNA in the 40 % PEG solution is under compressive pressure.

The contribution of PEG to the scattering

The incident wavelength was then changed to 4.61 Å, meaning that the intensity dip due to the cassette attenuation moved to larger $|Q|$ and the $Q_H \sim 1.87$ Å^{-1} Bragg peak line shape could be more reliably measured and fitted.

PEG is a long-chain molecule and, aside from adding substantial incoherent scattering, its presence will add some coherent scattering which might interfere with any attempt to quantitatively analyse the Bragg peaks. Measurements were thus made on an aluminium cassette containing only 26 % PEG solution with roughly the same volume as that used for the samples. A comparison of the intensity along the Q_H axis for this cassette and for the 17% PEG sample is shown in figure 5.

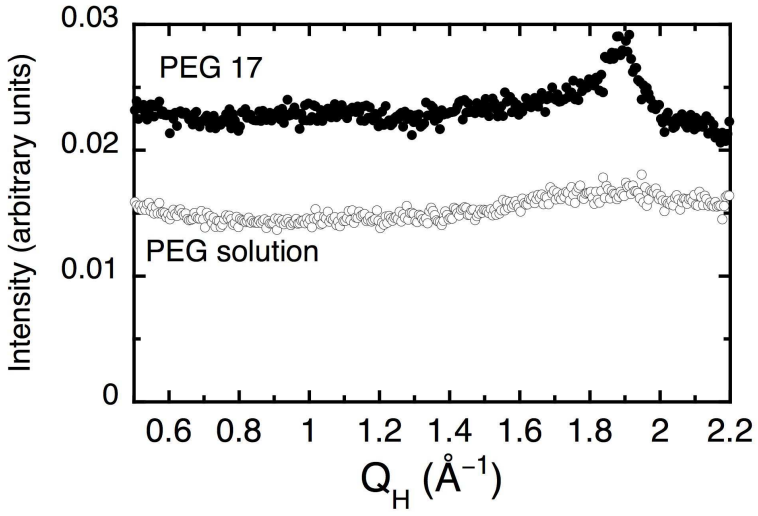

Figure 5: A cut along the Q_H axis for DNA in a 17% PEG solution, and for a cassette containing only the 26 % PEG solution. The data share the same axes.

The figure shows that the PEG solution accounts for the increase in the incoherent scattering. It has a weak Q dependence with a slight rise in the scattering at small Q and a broad maximum at $\sim$ 1.9 Å^{-1}, but the effect on the shape and intensity of the DNA Bragg peak is negligible. The coherent contribution of the PEG can thus be safely ignored in subsequent treatments of the Bragg peak.

Temperature dependence

Measurements of the temperature-dependent scattering from the 17 % PEG sample were made using 4.61 Å incident neutrons. Reciprocal space maps of the (Q_H, Q_K) plane were made at a range of temperatures from 300 K to 376 K. The measurement was stopped at 376 K due to concerns that the sample might boil at higher temperatures. The sample was then cooled back to 300 K and measured again.

Measuring reciprocal space maps had the advantage that the incoherent scattering background, and the influence of intensity dips due to the attenuation by the sample cassette, could be estimated by fitting a peak function with a negative amplitude and a flat background to the scattering far from any coherent contributions. The background estimation was made from the initial measurement at 300 K, and was then subtracted from the data at all temperatures.

Figure 6 shows examples of the resulting estimation of the coherent scattering along the Q_H axis at a number of temperatures. The data points show the detector intensities within $-0.05 \leq Q_K \leq 0.05$ Å^{-1} projected onto the Q_H axis. The data at 300 K show a clear peak on a non-zero background, indicating that some diffuse coherent scattering remains along the Q_H axis after the incoherent contribution has been subtracted. The origin of the diffuse scattering is not clear, but could be due to an increase in the orientational disorder in the fibres. Broad low-Q scattering is apparent in x-ray diffraction measurements on non-oriented fibres,[7] and in calculations of the neutron cross-section from partially disordered fibres. Both the peak and the diffuse scattering are temperature-dependent.

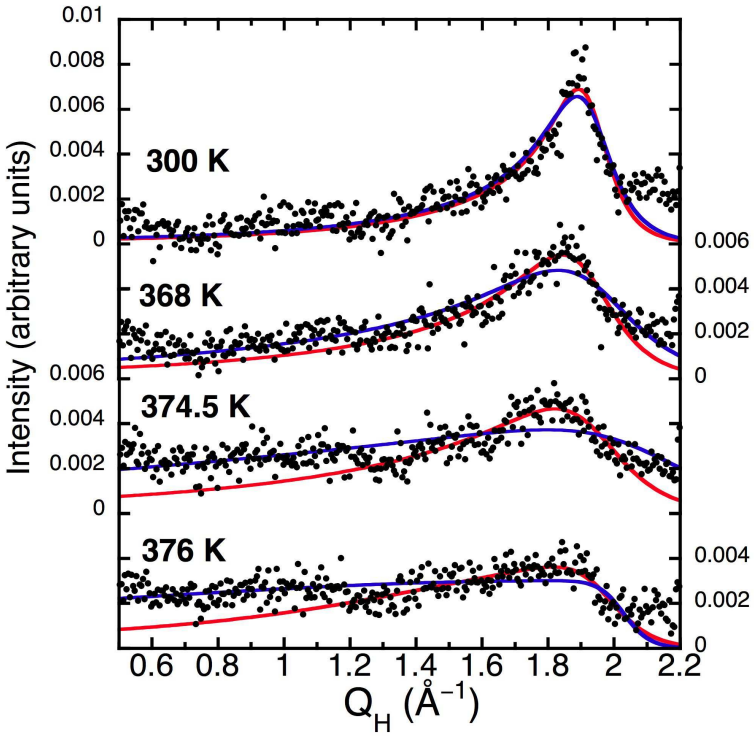

Figure 6: The temperature dependence of the $Q_H \approx 1.87$ Å^{-1} Bragg peak for the PEG 17 sample. The data have had the incoherent contributions subtracted. Fits of equation 3 for $0.5 \leq Q_H \leq 2.05$ Å^{-1} (blue curve) and $1.3 \leq Q_H \leq 2.05$ Å^{-1} (red curve) are shown superimposed on the data.

While the data clearly change with temperature, a quantitative analysis is not possible without a robust function to describe the structure factor. Unfortunately, the quality of the data will not support analysis using a detailed theoretical modelling of the structure factor. Examination of the integrated intensities, however, does give a qualitative indication of whether melting is occurring.

The summed data from figure 6 for a series of Q_H ranges are shown in figure 7. Integrating the data over the entire usable Q_H range gives a curve that increases with increasing temperature. No clear feature emerges to indicate the onset of melting. The initial integrated intensity was recovered when the sample was cooled back to 300 K from its highest temperature.

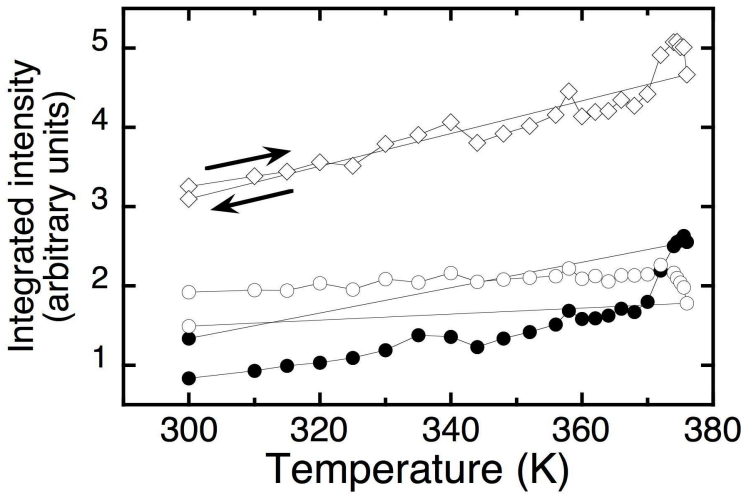

Figure 7: The integrated intensities along the Q_H axis for $0.5 \leq Q_H < 1.3$ Å^{-1} (closed circles); $1.3 \leq Q_H \leq 2.05$ Å^{-1} (open circles); $0.5 \leq Q_H \leq 2.3$ Å^{-1} (open diamonds). The sample was heated from 300 K to 376 K, and then cooled back to 300 K directly. The arrows show the directions of the temperature ramp for the data points at 300 K.

Features do emerge when some effort is made to separate the peak from the diffuse intensities. Inspection of the data in figure 6 shows an indication of a small dip at $Q_H \sim 1.3$ Å^{-1}, particularly at the highest temperatures. This point was arbitrarily set as a boundary, although the choice is reinforced by the observation that x-ray measurements on non-aligned fibres[7] and neutron scattering calculations on partially aligned fibres also show a dip at

around the same Q_H. The integrated intensities for the regions above and below the boundary are also plotted in figure 7. The figure shows that the steady rise in the total integrated intensity is almost entirely due to the scattering for $Q_H < 1.3$ Å^{-1}, which is taken to be only diffuse. The intensity for $Q_H > 1.3$ Å^{-1}, which includes the peak, stays almost constant over most of the temperature range. The data in figure 6 clearly show that the peak amplitude decreases with increasing temperature, however an overall gain in the diffuse scattering and a probable increase in the peak width would compensate for the decrease in peak amplitude to keep the $Q_H > 1.3$ Å^{-1} data roughly constant.

A sudden change in gradient for both Q_H regions is observed for $T > 370$ K. The low Q_H data shows a rapid increase while the high Q_H data shows a concomitant rapid decrease. The high Q_H data are consistent with the onset of melting, which would give rise to a loss in the peak intensity as observed in the past for both A- and B-form DNA.[3,4,7] The increase in the scattering at small Q_H is consistent with an increase in the disorder of the molecule. The possible sources of the disorder include local fluctuations in the alignment of the double-stranded DNA within the fibre, and the formation of single-stranded DNA on thermal denaturation.

On cooling to 300 K, figure 7 shows that there is some loss in the integrated intensity at high Q_H and a gain at low Q_H relative to the values before heating. A peak is, however, recovered. Figure 8 shows the scattering at 300 K before and after heating the sample. The data show a clear peak which is less intense after heating, while the low Q_H data is systematically higher.

Ideally, a quantitative analysis would include an estimate of the peak width allowing the correlation length to be plotted as a function of temperature. While the data will not support a fully robust analysis, they will support a semi-quantitative analysis with a phenomenological function:

$$I(Q) = \frac{I_0}{\pi} \cdot \frac{\Gamma^2(Q)}{(Q - Q_c)^2 + \Gamma^2(Q)}, \tag{3}$$

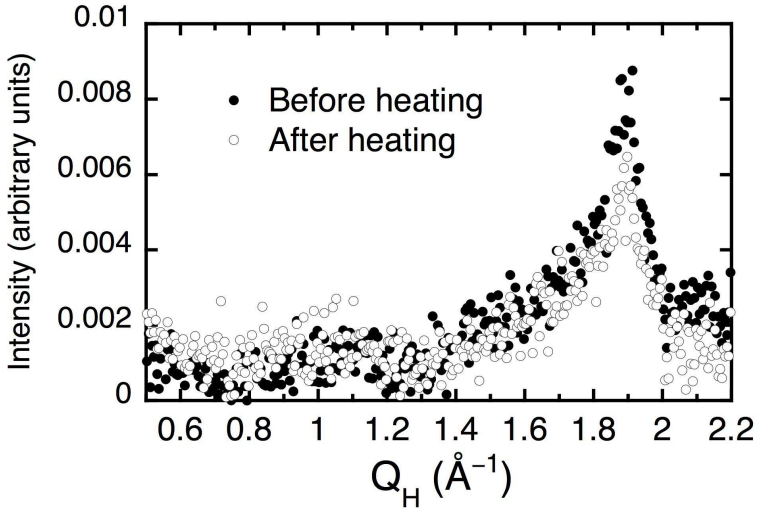

Figure 8: The $Q_H \approx 1.87$ Å^{-1} Bragg peak from the PEG 17 sample measured at 300 K before and after heating the sample to 376 K.

where $I(Q)$ is the intensity as a function of Q, Q_c is the centre for the peak and I_0 is the amplitude. The Q-dependent width is given by:

$$\Gamma(Q) = \frac{\Gamma_0}{1 + \exp(a(Q - Q_c))}, \tag{4}$$

where Γ_0 is a width and a is an asymmetry parameter. A value of $a = 0$ would reduce equation 3 to a symmetric function. The function is similar to an asymmetric Lorentzian derived for infrared spectrometry,[25] but has been modified such that it does not have a discontinuity at $Q = Q_c$.

Figure 6 shows fits of equation 3 superimposed on the data. Initial attempts to fit the data over the entire Q_H regime did not give robust results, as the increase in the diffuse scattering then dominated the fits. This is apparent by observing the blue lines in figure 6. The data were then fitted over a smaller range of $1.3 \leq Q_H \leq 2.05$ Å^{-1} to focus on the temperature-dependent behaviour of the peak. The lower limit corresponds to the previously set boundary for the integrated intensities, and the upper limit was chosen to avoid interference with the intensity dips due to the sample geometry. These fits better represented the changes in the peak shape, as can be seen by comparing the data with the red curves in figure 6. The Q_H

ranges could be adjusted by 10 % with little qualitative difference in the results.

The fit results are shown in figure 9. All the data have a linear trend with increasing temperature up to $T \sim 370$ K, with I_0, Q_c and a steadily decreasing and Γ_0 steadily increasing.

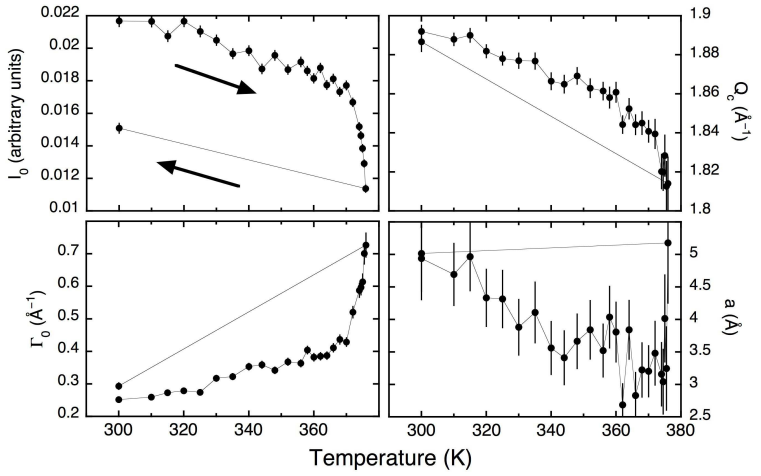

Figure 9: The fitted parameters for the $Q_H \approx 1.87$ Å^{-1} Bragg peak from the PEG 17 sample. The arrows show the direction of the temperature change between data points.

A sudden and dramatic change is clearly seen at $T \sim 370$ K in I_0 and Γ_0. The amplitude, I_0, plummets by ~ 40 % between 370 and 376 K, while Γ_0 increases by ~ 75 %. Much smaller changes in this temperature range are seen in Q_c, which drops by ~ 1 % between 372 and 374 K and then stays roughly constant, and a, which stays roughly constant except for the highest temperature. The change in I_0 is consistent with the loss in Bragg peak intensity observed at the onset of melting in both A- and B-form fibre DNA.[3,4,7] The increase in Bragg peak width is an expected, but never before definitively seen, indication of the decrease of the coherence length along DNA due to the formation of local openings, or "bubbles". That Γ_0 changes almost independently of a suggests that the peak width is independent of its asymmetry, and hence that a correlation length is changing in the sample over this temperature range.

With the exception of I_0, all the parameters are recovered on cooling the sample back to 300 K from 376 K. The parameters thus prove that the peak shape before and after cooling is the same, suggesting that the correlation length is restored on cooling the sample and

that the loss in the peak intensity is due to some loss in the quantity of the sample that is coherently diffracting.

Discussion

Immersing highly oriented fibre DNA in a PEG solution clearly leads to a degradation in the quality of the Bragg peaks. Some of the degradation may be due to a loss in the orientation and base pair stacking in the molecules. This may mean that a substantial fraction of the sample was not contributing to the Bragg peak intensity. A Bragg peak remains, however, meaning that quantitative experiments are possible despite the complications associated with the inclusion of a solution in the sample. A great advantage of focusing on the Bragg peak is that it arises due to those regions of B-form DNA that are scattering coherently with respect to one another. Hence, the Bragg peak signal effectively acts as a self-filter, probing the correlation function of those parts of the sample that give the most information and suppressing the rest.

The results shown in figures 6, 7, and 9 are consistent with the onset of the melting transition at $\sim$ 370 K, causing the coherent scattering intensity of the Bragg peak to be redistributed into the diffuse scattering. The recovery of the peak shape on cooling indicates that the DNA had not completely melted by 376 K and was able to recombine, although there was a reduction in the peak amplitude. The peak shape before and after heating was the same, indicating that the fibre alignment remained largely unchanged throughout the heating process. The temperature dependence of the scattering is consistent with the calorimetry data shown in figure 2. All the results suggest that the application of osmotic pressure is a viable technique for investigation of the effects of spatial confinement on the melting process of fibre DNA.

The statement that the fibre alignment stays mostly unchanged on heating has important consequences in the interpretation of the data and deserves further discussion. The

Bragg peak shape showed quantitative changes at the highest temperatures. Single strand DNA, created by local openings of the double helix on heating, is far more flexible than double strand and entropic effects could lead to substantial disorder, even to the point of the entire fibre undergoing macroscopic collapse. It is highly unlikely that substantial disorder at elevated temperatures would be undone when the temperature of the sample was cooled. Such a fibre collapse was observed in a previous study of highly oriented B-form Li-DNA[2,3] and non-oriented Na-DNA,[7] where subsequent diffraction measurements at reduced temperatures did not recover the original peak shape. The strong entropic effect associated with the growth of the melted regions also led to a visible decrease in the length of the fibre,[3] which was also seen in mechanochemical experiments.[26] As shown in figure 9, the values for Γ and a are essentially unchanged before and after heating. These parameters determine the peak shape and hence the spatial correlation length of double stranded DNA along the molecule. This correlation length is recovered in the present study, thus the DNA has recombined after heating. There is a loss of ~ 30 % in I_0 before and after heating which indicates that a fraction of the sample has either lost alignment or not recombined, and quite probably a combination of the two. However majority of the sample must have maintained its orientation throughout the heating process.

Supporting evidence comes from the calorimetry data in figure 2. Calorimetry measurements on "dry" fibres show that fibre DNA becomes glass-like after the melting transition,[21] consistent with the observed collapse of the fibre structure and the associated disorder of single-stranded DNA at elevated temperatures. In contrast, the data in figure 2 show transitions on consecutive temperature cycles, implying that a fraction of the denatured single strand DNA has maintained proximity to its opposite strand and is thus able to recombine on cooling.

The changes in Γ_0 at elevated temperatures, shown in figure 9 must therefore be dominated by a reduction in the spatial correlation length along the DNA molecule. They occur at around the same temperatures as the changes in I_0. The previous studies of "dry" fi-

bres observed a drop in I_0 well before any changes in the width, leading to the conclusion that the DNA must maintain long lengths of double strand structure until the final stages of melting.[2–4,7] The current study suggests that this conclusion may be a consequence of confinement.

Two recent publications describe theories to describe the influence of confinement on the melting transition in DNA. Chersty and Kornyshev[27] have included electrostatic interactions between DNA molecules. Their results depend strongly on the nature of the sequences. For homologous sequences, they predict that confinement makes the transition sharper and moves it to higher temperatures. For non-correlated sequences, which corresponds to our samples of genomic DNA, their conclusions are less clear and depend on the rigidity of the molecules. Badasyan and co-workers[28] explicitly consider the effects of PEG on the melting of DNA and find that an increase in the osmotic pressure increases the melting temperature and makes the transition smoother. The data in figure 2 certainly show that the melting transition for the"dry" fibre is much sharper than the less dense PEG 10 fibre. However, in contrast to the theory, the melting transition for the PEG 10 is at the higher temperature.

There are numerous possible reasons for the discrepancy, including the absence of a solvent in the "dry" sample with a concomitant mobility of salt cations. Thermal measurements of DNA in PEG solutions with the same salinity and different osmotic pressures provide a better test. Some experiments have been performed using techniques such as UV absorption, circular dichroism and differential scanning calorimetry,[15–18] which provide bulk information on the melting temperatures and enthalpies. The results presented here show that it is possible to carry out diffraction experiments on similar samples, hence providing additional information in the form of a correlation length. If the theories were to be revisited to calculate the temperature dependence of the correlation length, these diffraction experiments would be ideal to test them.

The experiment must certainly be refined to perform a quantitative analysis of the data in the same manner as has been performed previously.[2–4,7] There are numerous possible

improvements that will be explored in the future. Using PEG with lower molecular weight will lower the melting temperature,[15,18] which will mean that the entire melting transition can be followed without the risk of the sample boiling. While expensive, use of deuterated PEG would reduce the incoherent scattering and improve the signal-to-noise. The PEG solutions might be replaced by other solutions, such as ethanol/water,[26] that would have the same effect of increasing the intermolecular spacing while maintaining the highly oriented fibre structure of the DNA. Assuming that the signal can be improved, it will also be necessary to establish a representative and properly normalized function for the structure factor. These possibilities will be explored in future studies.

Conclusions

Calorimetry and diffraction experiments on the melting transition of fibre DNA subjected to osmotic pressure have been shown to be feasible. The pilot study shows a diffuse contribution to the scattering that grows with temperature as the Bragg peaks decrease. It appears to be possible to follow the melting transition to higher relative temperatures than can be reached when using "dry" fibres and, unlike for the latter samples, the transition appears to be reversible to some degree. The study highlights a number of issues that must be overcome in future experiments, namely in optimizing the signal such that the scattering can be reliably fitted with a temperature-dependent structure factor. Some possibilities for optimization have been presented.

Acknowledgement

The authors thank ANSTO for the beam time. AW performed this work while on sabbatical at ANSTO and thanks ANSTO for financial support.

References

(1) Peyrard, M. Nonlinear Dynamics and Statistical Physics of DNA. *Nonlinearity* **2004**, *17*, R1–R40.

(2) Wildes, A.; Theodorakopoulos, N.; Valle-Orero, J.; Cuesta-López, S.; Garden, J.-L.; Peyrard, M. Thermal Denaturation of DNA Studied with Neutron Scattering. *Phys. Rev. Lett.* **2011**, *106*, 048101.

(3) Wildes, A.; Theodorakopoulos, N.; Valle-Orero, J.; Cuesta-López, S.; Garden, J.-L.; Peyrard, M. Structural Correlations and Melting of B-DNA Fibers. *Phys. Rev. E* **2011**, *83*, 061923.

(4) Valle-Orero, J.; Wildes, A. R.; Theodorakopoulos, N.; Cuesta-López, S.; Garden, J.-L.; Danilkin, S.; Peyrard, M. Thermal Denaturation of A-DNA. *New J. Phys.* **2014**, *16*, 113017.

(5) Peyrard, M.; Bishop, A. R. Statistical Mechanics of a Nonlinear Model for DNA Denaturation. *Phys. Rev. Lett.* **1989**, *62*, 2755–2758.

(6) Dauxois, T.; Peyrard, M.; Bishop, A. R. Dynamics and Thermodynamics of a Nonlinear Model for DNA Denaturation. *Phys. Rev. E* **1993**, *47*, 684–695.

(7) Sebastiani, F.; Pietrini, A.; Longo, M.; Comez, L.; Petrillo, C.; Sacchetti, F.; Paciaroni, A. Melting of DNA Nonoriented Fibers: A Wide-Angle X-ray Diffraction Study. *J. Phys. Chem. B* **2014**, *118*, 3785–3792.

(8) Rau, D. C.; Lee, B.; Parsegian, V. A. Measurement of the Repulsive Force Between Polyelectrolyte Molecules in Ionic Solution: Hydration Forces Between Parallel DNA Double Helices. *Proc. Nat. Acad. Sci. USA* **1984**, *81*, 2621–2625.

(9) Podgornik, R.; Strey, H. H.; Rau, D.; Parsegian, V. A. Watching Molecules Crowd: DNA Double Helices Under Osmotic Stress. *Biophys. Chem.* **1995**, *57*, 111–121.

(10) Podgornik, P.; Strey, H. H.; Gawrisch, K.; Rau, D. C.; Rupprecht, A.; Parsegian, V. A. Bond Orientational Order, Molecular Motion, and Free Energy of High-density DNA Mesophases. *Proc. Natl, Acad Sci. USA* **1996**, *93*, 4261–4266.

(11) Yasar, S.; Podgornik, R.; Valle-Orero, J.; Johnson, M.; Parsegian, V. A. Continuity of States Between the Cholesteric to Line Hexatic Transition and the Condensation Transition in DNA Solutions. *Sci. Rep.* **2014**, *4*, 6877.

(12) Knowles, D. B.; LaCroix, A. S.; Deines, N. F.; Shkel, I.; Record, M. T. Separation of Preferential Interaction and Excluded Volume Effects on DNA Duplex and Hairpin Stability. *Proc. Natl, Acad Sci. USA* **2011**, *108*, 12699–12704.

(13) Nakano, S.; Yamaguchi, D.; Tateishi-Karimata, H.; Miyoshi, D.; Sugimoto, N. Hydration Changes upon DNA Folding Studied by Osmotic Stress Experiments. *Biophys. J.* **2012**, *102*, 2808–2817.

(14) Politi, R.; Harries, D. Enthalpically Driven Peptide Stabilization by Protective Osmolytes. *Chem. Commun.* **2010**, *46*, 6449–6451.

(15) Spink, C. H.; Chaires, J. B. Effects of Hydration, Ion Release, and Excluded Volume on the Melting of Triplex and Duplex DNA. *Biochem.* **1999**, *38*, 496–508.

(16) Goobes, R.; Kahana, N.; Cohen, O.; Minsky, A. Metabolic Buffering Exerted by Macromolecular Crowding on DNA-DNA Interactions: Origin and Physiological Significance. *Biochem.* **2003**, *42*, 2431–2440.

(17) Karimata, H.; Nakano, S.; Sugimoto, N. Effects of Polyethylene Glycol on DNA Duplex Stability at Different NaCl Concentrations. *Bull. Chem. Soc. Jpn.* **2007**, *80*, 1987–1994.

(18) Spink, C. H.; Garbett, N.; Chaires, J. B. Enthalpies of DNA Melting in the Presence of Osmolytes. *Biophys. Chem.* **2007**, *126*, 176–185.

(19) Rupprecht, A. Preparation of Oriented DNA by Wet Spinning. *Acta Chemica Scand.* **1966**, *20*, 494–504.

(20) Rupprecht, A. A Wet Spinning Apparatus and Auxiliary Equipment Suitable for Preparing Samples of Oriented DNA. *Biotech. Bioeng.* **1970**, *XII*, 93–121.

(21) Valle-Orero, J.; Garden, J.-L.; Richard, J.; Wildes, A.; Peyrard, M. Glassy Behavior of Denatured DNA Films Studied by Differential Scanning Calorimetry. *J. Phys. Chem. B* **2012**, *116*, 4394–4402.

(22) Valle-Orero, J.; Wildes, A.; Garden, J.-L.; Peyrard, M. Purification of A-Form DNA Fiber Samples by the Removal of B-Form DNA Residues. *J. Phys. Chem. B* **2013**, *117*, 1849–1856.

(23) Rand, R. P. http://www.brocku.ca/researchers/peter_rand/osmotic/data/peg20000.

(24) Avdeev, M.; Hester, J. R.; Peterson, V. K.; Studer, A. J. Wombat and Echidna: The Powder Diffractometers. *Neutron News* **2009**, *20*, 29–33.

(25) Stancik, A. L.; Brauns, E. B. A Simple Asymmetric Lineshape for Fitting Infrared Absorption Spectra. *Vibr. Spectr* **2008**, *47*, 66–69.

(26) Rupprecht, A.; Piskur, J.; Schultz, J.; Nordenskiöld, L.; Song, Z.; Lahajnar, G. Mechanochemical Study of Conformational Transitions and Melting of Li-, Na-, K-, and CsDNA Fibers in Ethanol-Water Solutions. *Biopolymers* **1994**, *34*, 897–920.

(27) Cherstvy, A. G.; Kornyshev, A. A. DNA Melting in Aggregates: Impeded or Facilitated? *J. Phys. Chem. B* **2005**, *109*, 13024–13029.

(28) Badasyan, A.; Tonoyan, S.; Giacometti, A.; Podgornik, R.; Parsegian, V. A. Osmotic Pressure Induced Coupling between Cooperativity and Stability of a Helix-Coil Transition. *Phys. Rev. Lett.* **2012**, *109*, 068101.

Graphical TOC Entry